Nuclear Shadowing in the Holographic Framework

L. Agozzino,[1,2] P. Castorina,[1,2] and P. Colangelo[3]
[1]Dipartimento di Fisica, Universitá di Catania, via S. Sofia 62, 95125 Catania, Italy
[2]INFN, Sezione di Catania, via S. Sofia 62, 95125 Catania, Italy
[3]INFN, Sezione di Bari, via Orabona 4, 70126 Bari, Italy

(Received 26 June 2013; revised manuscript received 30 October 2013; published 31 January 2014)

The nucleon structure function F_2^N computed in a holographic framework can be used to describe nuclear deep inelastic scattering effects provided that a rescaling of the Q^2 momentum and of the IR hard-wall parameter z_0 is made. The ratios $R_A = F_2^A/F_2^N$ can be obtained in terms of a single rescaling parameter λ_A for each nucleus. The resulting ratios agree with the experiment in a wide range of the shadowing region.

DOI: 10.1103/PhysRevLett.112.041601 PACS numbers: 11.25.Tq, 11.10.Kk, 12.38.Lg, 24.85.+p

Introduction.—The AdS/CFT correspondence [1], an important tool to analyze nonperturbative aspects of gauge theories, has been successfully used to study features of QCD [2]. In its application to deep inelastic scattering (DIS) at strong coupling [3,4], the nucleon structure function $F_2^N(x, Q^2)$ at small Bjorken variable x has been represented as the sum of a conformal term and of a contribution due to quark confinement, crucial to fit the data. The evaluation of these contributions requires the holographic nucleon wave function, which is assumed to be peaked at distances $O(1/Q')$ close to the infrared boundary z_0, with Q' of the order of the nucleon mass.

Nonperturbative, confinement dynamics shows up also in the modification of the structure functions of a nucleon in a nucleus. The proposed theoretical models of these effects are based on the effective change of the mean square distances among quarks and gluons in a nuclear environment with respect to the free nucleon case [5].

Nuclear effects are described comparing the structure functions of the nuclear target per nucleon to the free nucleon ones and, for electroproduction, the ratios $R_A = F_2^A(x, Q^2)/F_2^D(x, Q^2)$ are considered, with F_2^A and F_2^D the structure functions per nucleon in the nucleus A and in deuterium D (where the nuclear binding is considered negligible). Nuclear modifications depend on x: $x \leq 0.1$ is the shadowing region where $R_A < 1$; for large x one has the so-called EMC effect; in the range $0.1 < x < 0.25$ there is the antishadowing with $R_A > 1$, usually obtained by the energy-momentum sum rule. The understanding of these modifications requires to evaluate the "distortion" of the free nucleon wave function due to nuclear binding. In the small-x region, dominated by Pomeron exchange, the AdS/CFT strong coupling BPST Pomeron kernel [6] is a good framework to study nuclear deep inelastic structure functions, provided one knows the holographic baryon wave function in the nucleus. A simplified approach can be based on the observation that the spatial separation between quarks determines the strength of the quark-Pomeron coupling [7] and that the effective confinement size is modified in a nucleus.

Following this point of view, we consider an approach to shadowing in an AdS/CFT framework, describing the nuclear binding effects on the nucleon wave function through an effective distance $1/Q'_A$ and an effective confinement boundary z_0^A, and studying the scaling properties of the holographic structure function F_2 under the change $Q' \to Q'_A$ and $z_0 \to z_0^A$. In this way, nuclear effects are described by rescaling the confinement parameters. The results agree with the experimental data.

Approaches to nuclear DIS effects.—In models of shadowing and EMC effects, the description of the nuclear modifications is based on the change of the effective mean square distance among quarks and gluons in a nuclear environment with respect to the free nucleon case [5].

In the x-rescaling model the EMC effect is described by rescaling x in the free nucleon structure function [8],

$$F_2^A(x, Q^2) = F_2^D(x/\hat{z}, Q^2), \tag{1}$$

with $\hat{z} \simeq 1 - \epsilon/M$, M the proton mass and ϵ the energy necessary to "ionize" a nucleus and make it emit a nucleon. However, the values of ϵ able to fit the large-x data exceed the nuclear binding calculations [5].

The Q^2-rescaling model of the EMC effect is based on the relation [9,10]

$$F_2^A(x, Q^2) = F_2^D(x, \chi_A Q^2), \tag{2}$$

indicating that the effective Q^2 for a bound nucleon is different from the free nucleon. This dynamical property is investigated here in the holographic framework. It is related to the modification of the quark confinement size in the nucleus [9,10]: quarks and gluons are no longer confined to specific nucleons, but spread over distances larger than the free nucleon size. By studying the structure function moments, starting from a Q^2 region where the valence picture is a good approximation, one can show that in QCD, for large Q^2, this change of scale is connected to the strong coupling constant α_s. The x-and Q^2-rescaling models, although different in their starting points, can be related [11].

The QCD Q^2 dependence of structure functions can be also applied to shadowing at small x, including the effect of gluon recombination in nuclei which is neglected in the free nucleon evolution equation [12]. Modifying the linear Q^2 evolution equation one shows that the recombination depletes the gluon distribution at small x, which reflects into a depletion of sea quark distribution [12]. The Q^2 dependence of parton distributions in nuclei based on linear QCD evolution equations at next-to-leading order is described in Ref. [13].

A different nonperturbative approach considers that the small-x behavior of F_2 is controlled by Pomeron exchange [14]. In a nuclear environment the effective coupling of the Pomeron to a quark is suppressed because of the nucleon overlap. Although quarks and gluons are no longer confined to specific nucleons but rather spread on distances larger than the free nucleon size, the average spatial separation between quarks before color neutralization decreases, with the Pomeron coupling directly related with this typical size [7].

Hence, a physical description of EMC and shadowing effects can be based on the effective modification of the dynamical scales in deep inelastic scattering on nuclear target respect to the free nucleon case. This rescaling, and in particular the Q^2 one, is a property of the AdS/CFT approach to deep inelastic scattering, not only in the conformal limit but also if the confinement dynamics is taken into account.

Nuclear structure functions in a holographic framework.—The possibility of an approach to DIS on a proton based on AdS/CFT duality was analized in the Polchinski-Strassler first proposal [3]. Here we adopt the method in [4], based on the calculation of the virtual $\gamma^* p$ total cross section, which allows us to express, e.g., the structure function F_2 as the sum of two contributions: a model-independent term for conformal gauge theories and an additional nonconformal term accounting for confinement. This latter (model-dependent) contribution is obtained by breaking conformal invariance through a sharp cutoff ("hard wall") of the AdS holographic space [15].

One starts from the matrix element of two R currents in a hadron of momentum P and charge $\mathcal{Q}$,

$$T^{\mu\nu} \equiv i \int d^4y e^{iq\cdot y} \langle P\mathcal{Q}|T[J^\mu(y)J^\nu(0)]|P\mathcal{Q}\rangle = F_1(x,Q^2)\left(\eta^{\mu\nu} - \frac{q^\mu q^\nu}{q^2}\right) + \frac{2x}{q^2}F_2(x,Q^2)\left(P^\mu + \frac{q^\mu}{2x}\right)\left(P^\nu + \frac{q^\nu}{2x}\right), \quad (3)$$

(with μ, ν four-dimensional indices, $\eta^{\mu\nu}$ Minkowski metric, $x = Q^2/2Pq$ and $Q^2 = -q^2$), which allows us to extract the DIS structure functions for electron-hadron scattering and, in particular, $F_2(x,Q^2)$. The AdS/CFT calculation involves the couplings

$$g_s = \frac{g_{YM}^2}{4\pi} = \alpha_{YM} = \frac{\lambda}{4\pi N_C}, \qquad R = \alpha'^{(1/2)}\lambda^{(1/4)} \quad (4)$$

with $g_s \ll 1$ and $\lambda \gg 1$. R is the AdS radius. In the following, the coupling $\rho = 2/\sqrt{\lambda}$ is used.

The dual string calculation of the matrix element (3), or of its imaginary part appearing in DIS processes, describes the scattering in the AdS space, and involves various quantities. First, to describe the transition $\gamma^* N \to \gamma^* N \equiv 1,2 \to 3,4$, states dual to the initial-final nucleon N are required, i.e., the hadronic state $|PQ\rangle$ in (3). These states are represented by normalizable wave functions $\phi^N(z)$ depending on the holographic coordinate z (positive and with the UV brane corresponding to $z = 0$), and are obtained in principle from a suitable equation of motion. The calculation of the matrix element (3) involves the transition function

$$P_{24}(z) = \sqrt{-g}\left(\frac{z}{R}\right)^2 \varphi^N(z)\varphi^N(z). \quad (5)$$

The current that couples to the hadrons in (3) induces non-normalizable modes of the gauge fields. In the bulk, such fields $\mathcal{A}$ satisfy Maxwell's equations of motion; their solutions, in the Lorentz gauge and for $R = 1$, are given in terms of Bessel functions: $\mathcal{A}_\mu(y,z) = n_\mu(Qz)K_1(Qz)e^{iq\cdot y}$ and $\mathcal{A}_z(y,z) = i(q\cdot n)(Qz)K_0(Qz)e^{iq\cdot y}$, with n_μ a polarization vector. To determine the structure function F_2 in (3) a transition function P_{13} is needed, and is given by [4,16]

$$P_{13}(z,Q^2) = \frac{1}{z}(Qz)^2[K_0^2(Qz) + K_1^2(Qz)] \quad (6)$$

with $Q = \sqrt{Q^2}$.

The last ingredient is the scattering kernel. This has been expressed in terms of a Pomeron Regge pole contribution [6], and allows us to write the structure function F_2 at low x as an eikonal sum with a convolution of the transition functions (5) and (6) [4]:

$$F_2^N(x,Q^2) = \frac{Q^2}{2\pi^2}\int d^2b \int dz dz' P_{13}(z,Q^2)P_{24}(z') \times \mathrm{Re}(1 - e^{i\chi(s,b,z,z')}). \quad (7)$$

b is the impact parameter, with $\vec{b}$ the transverse Minkowski space vector for $\gamma^* p$ scattering; s is the center-of-mass energy squared of the γ^*-target system. The eikonal χ can be derived for conformal theories; it can also be modified by the inclusion of conformal symmetry-violating effects.

Conformal limit:—For conformal fields the free nucleon structure function F_2^N can be obtained from (7) and is given by [4]

$$F_2^N(x,Q^2) = \frac{g_0^2\rho^{3/2}}{32\pi^{5/2}}\int dz dz' \frac{zz'Q^2}{\tau^{1/2}} P_{13}(z,Q^2)P_{24}(z') \times e^{(1-\rho)\tau}\exp\,[\Phi(z,z',\tau)], \quad (8)$$

where $x \simeq Q^2/s$ and g_0^2 a constant. The conformal invariant τ is defined as $\tau = \log(\rho z z' s/2)$. The function Φ is the BPTS Pomeron kernel integrated in the impact parameter [6],

$$\Phi(z, z', \tau) = -\frac{(\log z - \log z')^2}{\rho\tau}. \quad (9)$$

The transition function P_{24} involves the nucleon wave function in the bulk $\phi^N(z)$. In Ref. [4] it is assumed that the wave function $\phi^N(z)$ is sharply peaked near the infrared boundary z_0, with $1/Q' \leq z_0$ and Q' close to the nucleon mass,

$$P_{24}(z') \simeq \delta(z' - 1/Q'), \quad (10)$$

an expression adopted in the following. An explicit bulk model for the nucleon would be required to improve the wave function profile; modifications of this local approximation can be considered [17]. A further simplification consists in replacing also P_{13} by a local expression,

$$P_{13}(z, Q^2) \simeq C\delta(z - 1/Q), \quad (11)$$

with $C \simeq 1$. Since the integrand with P_{13} in Eq. (8) is peaked for $z \simeq 1/Q$, one can verify that this is a good approximation of Eq. (6). The resulting F_2 reads [4]

$$F_2^N(x, Q^2) = \frac{g_0^2\rho^{3/2}}{32\pi^{5/2}}\frac{Q}{Q'}\frac{1}{\tau^{1/2}}e^{(1-\rho)\tau}e^{-[\log^2(Q/Q')/\rho\tau]}. \quad (12)$$

The nucleon structure function F_2^A at small x in a nuclear environment can be obtained rescaling the effective size of the nucleon wave function in the nucleus A,

$$Q'_A = \lambda_A Q', \quad (13)$$

in Eq. (12). In the conformal limit F_2 depends on the ratio Q/Q'; therefore, the rescaling $Q'_A \to Q'$ corresponds to the Q^2 rescaling $Q^2 \to Q^2/\lambda_A^2$. Hence, in this limit one has $R_A = F_2^A/F_2^D$ neglecting the proton-neutron difference. Therefore, in the conformal limit the Q^2 rescaling at small x naturally arises in the AdS/CFT approach. This is not surprising, since the limit is reliable at large Q^2. Notice that in the local approximation (10,11), $\tau = \log(\rho Q/2xQ')$; therefore, the rescaling $Q'_A = \lambda_A Q'$ could be reabsorbed in $x \to \lambda_A x$. However, due to the Q^2 dependence of F_2 in Eq. (12), the x rescaling is not completely equivalent to the rescaling in Q^2, and $F_2^A(x, Q^2/\lambda^2) \neq F_2^A(\lambda x, Q^2)$. The x-rescaling method in the holographic framework will be discussed in a dedicated study [17].

Confinement effects:—The expression for F_2^N for the free proton structure functions, based on the conformal BPST Pomeron, does not fit the HERA data in the low Q^2 region, where confinement is the main dynamical mechanisms [4]. One needs to account for confinement, which can be described including an infrared boundary z_0 on the z coordinate of the bulk. This scale could be related to the $\Lambda_{\rm QCD}$ parameter. It produces a mass gap, a modification of the eikonal and a nonconformal contribution to F_2^N which, for a single Pomeron, reads [4]

$$F_{2cf}^N(x, Q^2, z_0) = \frac{g_0^2\rho^{3/2}}{32\pi^{5/2}}\int dz dz' \frac{z z' Q^2}{\tau^{1/2}} P_{13}(z, Q^2) P_{24}(z') \times e^{(1-\rho)\tau} e^{-\frac{\log^2(zz'/z_0^2)}{\rho\tau}} G(z, z', \tau). \quad (14)$$

In this expression the z_0 dependence is shown explicitly; $G(z, z', \tau)$ is given by

$$G(z, z', \tau) = 1 - 2\sqrt{\rho\pi\tau}e^{\eta^2} erfc(\eta), \quad (15)$$

and

$$\eta = \frac{-\log(zz'/z_0^2) + \rho\tau}{\sqrt{\rho\tau}}. \quad (16)$$

With the local approximation (10), (11), Eq. (14) reduces to

$$F_2^N(x, Q^2, Q_0^2) = \frac{g_0^2\rho^{3/2}}{32\pi^{5/2}}\frac{(Q/Q')}{\tau^{1/2}}e^{(1-\rho)\tau} \times e^{-\frac{\log^2(Q_0^2/(QQ'))}{\rho\tau}} G\left(\frac{1}{Q}, \frac{1}{Q'}, \tau\right), \quad (17)$$

where $Q_0 = 1/z_0$ [4].

In the description of nuclear effects by the rescaling $Q'_A = \lambda_A Q'$, the τ dependence on the ratio Q/Q' is remarkable, and would suggest a Q^2 rescaling. However, there is also a nontrivial Q^2 behavior in the log factors and in η due to the new scale Q_0. The dependence on Q_0 in Eq. (14) is in the form Q_0^2/QQ', and therefore the rescaling $Q'_A = \lambda_A Q'$ can be reabsorbed in the Q^2 rescaling $Q^2 \to Q^2/\lambda_A^2$ provided that the confinement distance in nuclear environment scales in the same way,

$$Q_0^2 \to Q_0^2/\lambda_A^2. \quad (18)$$

Our phenomenological analysis is done using this rescaling of Q_0 at fixed x.

Comparison with nuclear DIS data, comments, and conclusions.—The knowledge of structure functions and parton distribution functions in nuclei is important in relativistic heavy ion collisions, since the "hard probes" of the quark-gluon plasma require a control of cold nuclear effects, i.e., the modifications depending on the nuclear dynamics [13,18,19].

The results of the holographic approach can be compared to experimental data [20] by applying the Q^2 rescaling scheme based on Eqs. (12), (18): when $Q'_A = \lambda_A Q'$ one rescales $Q^2 \to Q^2/\lambda_A^2$ and $Q_0^2 \to Q_0^2/\lambda_A^2$. The Q^2 rescaling is exact not only in the conformal part but also in the confinement contribution. This implies

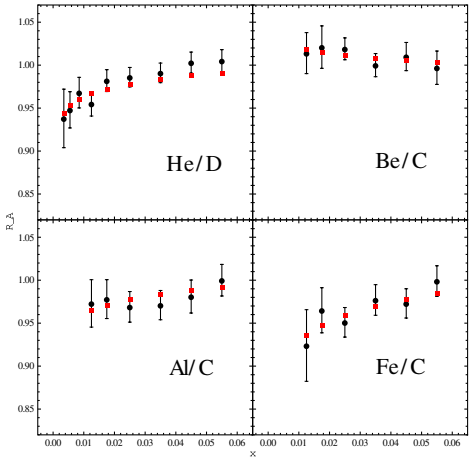

FIG. 1 (color online). Experimental data (black points) [20] and AdS/CFT results based on Q^2 rescaling (red squares) for various nuclei. The values of the experimental average Q^2 (in GeV^2), from the first to the last bin in x, vary in the ranges [0.77–6.3] (He/D), [3.4–9.8] (Be/C), [3.4–11.6] (Al/C), [3.4–11.8] (Fe/C). The theoretical values are obtained by Eq. (19) using the experimental average Q^2 for given x and the λ_A parameters in the first column of Table I. The χ^2/d.o.f. is 1.09 (He/D), 0.21 (Be/C), 0.23 (Al/C), and 0.41 (Fe/C).

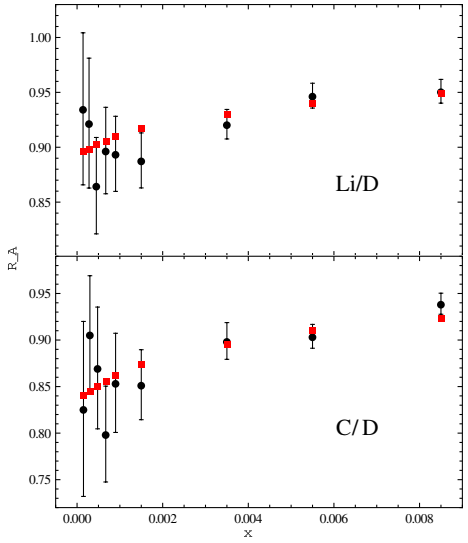

FIG. 2 (color online). Low-x experimental data for R_A (black points) [20] compared to holographic results (red squares) for different nuclei. The experimental average Q^2 (in GeV^2), from the first to the last bin in x, varies in the ranges [0.034–1.4] (Li/D), [0.035–1.6] (C/D). The theoretical values are obtained using Eq. (19) and the experimental average Q^2 for given x. The χ^2/d.o.f. is 0.93 (Li/D) and 1.61 (C/D).

$$F_2^A(x,Q^2) = F_{2,cl}^N\left(x,\frac{Q^2}{\lambda_A^2}\right) + F_{2,ct}^N\left(x,\frac{Q^2}{\lambda_A^2},\frac{Q_0^2}{\lambda_A^2}\right), \quad (19)$$

with the conformal term $F_{2,cl}^N$ in Eq. (12) and the confinement one $F_{2,ct}^N$ in Eq. (17). For each nucleus there is only one parameter λ_A.

Figures 1 and 2 report the comparison of the theoretical results with NMC data [20] in the small-x region, $x \leq 0.07$, for different nuclei. The theoretical values are obtained using the average Q^2 for a given x, the other parameters being fixed as in [4]. The agreement with data is remarkable, despite the neglect of the proton and neutron structure function difference. The optimization of the parameters λ_A and a complete analysis is presented elsewhere [17]; considering the neutron-proton isospin breaking improves the χ^2/d.o.f.

Understanding the agreement of the holographic result with nuclear data is easier if we consider the origin of (13) and (18). In the AdS/CFT framework, this comes from the identification of the bulk coordinate with the energy scale of the dual theory: considering the form of the AdS metric in Poincaré coordinates, a coordinate rescaling $x_\mu \to \lambda x_\mu$ on the boundary corresponds to $z \to \lambda z$ in the bulk. In nuclei, due to the nucleon overlap, the average distance among quarks and gluons decreases and the color neutralization infrared (confinement) scale increases. Such modifications in the boundary correspond in the bulk, respectively, to $z' \to z'/\lambda$ and $z_0 \to \lambda z_0$, i.e., the prescription employed to describe the nuclear effects by the momenta redefinition. The dynamical generation of the effective IR scale remains to be clarified, with a possible analogy with the generation of the saturation scale in free nucleon within this framework [21].

The method inspired by AdS/CFT provides a description of the nuclear effects in the DIS structure functions based on Q^2-rescaling which corresponds to a geometrical scaling of the confinement size for a bound nucleon. The same result can be obtained in other, rather different, frameworks. Indeed, at high energy, the structure functions can be evaluated in the QCD dipole model [22,23], where the virtual photon γ^* splits in a quark-antiquark dipole interacting with the target (T). Assuming, within this model, that the energy and target size dependence of the dipole-target cross section $\sigma^{\gamma^* T}$ can be encoded in a saturation scale $Q_{S,T}(x)$ [24], that there is no dependence of the dipole wave function on the quark and antiquark distribution of the longitudinal momenta [25], and that there is a minor dependence of the saturation scale on the specific scattering process, the dimensionless ratio $\sigma^{\gamma^* T}/\pi R_T^2$ depends only on $\tau_T^2 = Q^2/Q_{S,T}^2(x)$. The geometric scaling between the nucleus and the nucleon cross sections [24]

$$\frac{\sigma^{\gamma^* A}(\tau_A)}{\pi R_A^2} = \frac{\sigma^{\gamma^* N}(\tau_N)}{\pi R_N^2}, \quad (20)$$

with radii $R_{N,A}$ and

$$\tau_A^2 = \tau_N^2\left(\frac{\pi R_A^2}{A\pi R_N^2}\right)^{1/\delta}, \quad (21)$$

implies the relation

TABLE I. λ_A obtained using F_2 in the holographic approach, compared to the QCD dipole picture [24] and the change in the nucleus confinement size due to two-nucleon overlap [10].

A	λ_A (AdS/CFT)	$\lambda_{A,\mathrm{dip}}$ [24]	$\lambda_{A,\mathrm{nuc}}$[10]
Li	1.069	1.125	1.045
Be	1.073	1.128	1.077
C	1.111	1.143	1.104
Al	1.184	1.243	1.140
Ca	1.219	1.315	1.137
Fe	1.251	1.387	1.154
Pb	1.327	1.755	1.188

$$Q_{S,A}^2 = Q_{S,N}^2 \left(\frac{A\pi R_N^2}{\pi R_A^2}\right)^{1/\delta}. \tag{22}$$

The relation between the structure function per nucleon F_2^A and $\sigma^{\gamma^* A}/\pi R_A^2$ involves the factor $Q^2\pi R_A^2/A$, which can be approximated by $Q^2/Q_{S,A}^2$ if the x dependence of the saturation scale is neglected. As a result, the dependence of F_2^A on $Q^2/Q_{S,A}^2$ corresponds to rescaling $Q^2 \to Q^2/\lambda_{A,\mathrm{dip}}^2$, with

$$\lambda_{A,\mathrm{dip}} = \left(\frac{A\pi R_N^2}{\pi R_A^2}\right)^{1/2\delta}. \tag{23}$$

A good fit of low-x nuclear data in the dipole model is obtained for $R_A = (1.12A^{1/3} - 0.86A^{-1/3})$ fm, $\pi R_N^2 = 1.55$ fm^2 and $\delta = 0.79$ [24].

In Table I we compare the parameters λ_A obtained in the holographic framework and in the QCD dipole picture. Although the theoretical approaches are different, the deviation in this parameter is restrained in the range 5%–11% going from Li to Fe; for Pb the deviation is about 32%.

The rescaling $Q_0 \to Q_0/\lambda_A$ corresponds to the modification $z_0^A = \lambda_A z_0$, that is to an increase of the confinement size in nuclei. It is interesting to compare the results also with the changes in the confinement size in a nucleus $\lambda_{A,\mathrm{nuc}}$ evaluated by the overlap of two nucleons interacting by a Reid soft-core potential [10], reported in Table I. In this case the deviation on λ_A is between 4% and 8% from Li to Fe, and 12% for Pb.

The modification of the confinement sizes is a dynamical property of the bound nucleons, independent of x, which permits the description of nuclear effects at low x. On the other hand, at larger x one has the EMC and antishadowing regions. A general approach in the whole kinematical region $0 < x < 1$ is still lacking, but a Q^2 rescaling, although with different features for large and low x, could be the unifying dynamical element. We have found that, starting from a gauge-gravity duality approach, a reliable description of nuclear shadowing can be obtained rescaling the virtual photon scale Q^2 "seen" by a parton in a bound nucleon.

[1] J. M. Maldacena, Adv. Theor. Math. Phys. **2**, 231 (1998); [Int. J. Theor. Phys. **38**, 1113 (1999)]; S. S. Gubser, I. R. Klebanov, and A. M. Polyakov, Phys. Lett. B **428**, 105 (1998); E. Witten, Adv. Theor. Math. Phys. **2**, 253 (1998).

[2] See, e.g., J. Erlich, E. Katz, D. T. Son, and M. A. Stephanov, Phys. Rev. Lett. **95**, 261602 (2005); O. Aharony, J. Sonnenschein and S. Yankielowicz, Ann. Phys. (Amsterdam) **322**, 1420 (2007); J. Casalderrey-Solana, H. Liu, D. Mateos, K. Rajagopal, and U. A. Wiedemann, arXiv:1101.0618.

[3] J. Polchinski and M. J. Strassler, Phys. Rev. Lett. **88**, 031601 (2002); J. High Energy Phys. 05 (**2003**) 012.

[4] R. C. Brower, M. Djuric, I. Sarcevic, and C.-I Tan, J. High Energy Phys. 11 (**2010**) 051.

[5] M. Arneodo, Phys. Rep. **240**, 301 (1994).

[6] R. C. Brower, J. Polchinski, M. J. Strassler, and C.-I. Tan, J. High Energy Phys. 12 (**2007**) 005.

[7] B. Povh and J. Hufner, Phys. Rev. Lett. **58**, 1612 (1987).

[8] S. V. Akulinichev, S. A. Kulagin, and G. M. Vagradov, Phys. Lett. **158B**, 485 (1985); S. V. Akulinichev, S. Shlomo, S. A. Kulagin, G. M. Vagradov, Phys. Rev. Lett. **55**, 2239 (1985).

[9] F. E. Close, R. G. Roberts, and G. G. Ross, Phys. Lett. **129B**, 346 (1983); R. L. Jaffe, F. E. Close, R. G. Roberts, and G. G. Ross, Phys. Lett. **134B**, 449 (1984); R. L. Jaffe, Phys. Rev. Lett. **50**, 228 (1983).

[10] F. E. Close, R. L. Jaffe, R. G. Roberts and G. G. Ross, Phys. Rev. D **31**, 1004 (1985).

[11] F. E. Close, R. G. Roberts and G. G. Ross, Phys. Lett. **168B**, 400 (1986); R. P. Bickerstaff and G. A. Miller, Phys. Lett. **168B**, 409 (1986).

[12] A. H. Mueller and J.-w. Qiu, Nucl. Phys. **B268**, 427 (1986); J.-w. Qiu, Nucl. Phys. **B291**, 746 (1987).

[13] K. J. Eskola, H. Paukkunen and C. A. Salgado, J. High Energy Phys. 04 (**2009**) 065.

[14] P. Castorina and A. Donnachie, Phys. Lett. B **215**, 589 (1988); Z. Phys. C **45**, 141 (1989).

[15] For other ways of breaking the conformal invariance, see S. S. Gubser, arXiv:hep-th/9902155; U. Gursoy and E. Kiritsis, J. High Energy Phys. 02 (**2008**) 032; U. Gursoy, E. Kiritsis and F. Nitti, J. High Energy Phys. 02 (**2008**) 019.

[16] B. Pire, C. Roiesnel, L. Szymanowski, and S. Wallon, Phys. Lett. B **670**, 84 (2008).

[17] L. Agozzino, P. Castorina and P. Colangelo arXiv:1401.0826.

[18] K. J. Eskola, V. J. Kolhinen, H. Paukkunen and C. A. Salgado, J. High Energy Phys. 05 (**2007**) 002.

[19] A. Accardi, F. Arleo, N. Armesto, R. Baier, D. G. d'Enterria, R. J. Fries, O. Kodolova, and I. P. Lokhtin *et al.*, arXiv:hep-ph/0310274.

[20] P. Amaudruz *et al.* (New Muon Collaboration), Nucl. Phys. **B441**, 3 (1995); M. Arneodo *et al.* (New Muon. Collaboration), Nucl. Phys. **B441**, 12 (1995); M. Arneodo *et al.* (New Muon Collaboration), Nucl. Phys. **B481**, 3 (1996).

[21] L. Cornalba and M. S. Costa, Phys. Rev. D **78**, 096010 (2008); Y. Hatta, E. Iancu, and A. H. Mueller, J. High Energy Phys. 01 (**2008**) 026.

[22] N. N. Nikolaev and B. G. Zakharov, Z. Phys. C **49**, 607 (1991).

[23] A. H. Mueller, Nucl. Phys. **B415**, 373 (1994).

[24] J. L. Albacete, N. Armesto, J. G. Milhano, C. A. Salgado, and U. A. Wiedemann, Eur. Phys. J. C **43**, 353 (2005); J. L. Albacete, N. Armesto, J. G. Milhano, C. A. Salgado, and U. A. Wiedemann, Phys. Rev. D **71**, 014003 (2005).

[25] D. Schildknecht, Phys. Lett. B **716**, 413 (2012).